PALEOCEANOGRAPHY, VOL. 12, NO. 6, PAGES 729-741, DECEMBER 1997

# Pliocene carbonate accumulation along the California margin

A. C. Ravelo,[1] M. Lyle,[2] I. Koizumi,[3] J.P Caulet,[4] E. Fornaciari,[5]

A. Hayashida,[6] F. Heider,[7] J. Hood,[8] S. Hovan,[9] T. Janecek,[10] A. Janik,[8]

R. Stax,[11] M. Yamamoto,[12] and the ODP Leg 167 Shipboard Scientific Party.

**Abstract.** Recent modeling studies call on increased ocean heat transport to explain high-latitude warming observed for intervals throughout the middle Pliocene. Possible vehicles for ocean heat transport are the poleward arms of the sub-tropical gyres. Sites from the California margin (Ocean Drilling Program Leg 167) provide monitors of wind field within the eastern arm of the gyre which may be an indication of basin-wide subtropical gyral strength. At most sites (water depths from 1106 to 4212 m) $CaCO_3$ mass accumulation rate (MAR) was highest in the middle Pliocene (3.5-2.0 Ma). This high $CaCO_3$ MAR "event" is attributed primarily to higher $CaCO_3$ production due to higher offshore upwelling associated with the zone of the greatest wind stress curl. Thus, in the middle Pliocene, there was enhanced wind stress curl along the California margin, and possibly enhanced North Pacific sub-tropical gyral circulation and meridional ocean heat advection.

## 1. Introduction

Previous studies have demonstrated that intervals within the early to middle Pliocene were warmer than today in the Southern Ocean [*Ciesielski and Weaver*, 1974; *Ciesielski and Grinstead*, 1986; *Hodell and Kennett*, 1986; *Abelmann et al.*, 1990; *Hodell and Warnke*, 1991; *Hodell and Venz*, 1992; *Burkle*, 1996], in the North Atlantic [e.g. *Dowsett and Poore*, 1991; *Dowsett et al.*, 1992] and in the North Pacific [Barron, 1992a, b, 1995; *Heusser and Morley*, 1996]. Several modeling studies [e.g., *Rind and Chandler*, 1991; *Crowley*, 1996; *Sloan et al.*, 1996] have examined various mechanisms that may have produced Pliocene warmth and suggest that there may be a link, which should be tested with observational data, between intervals of high-latitude Pliocene warmth and meridional ocean heat transport. Meridional heat transport occurs in the surface water via the boundary currents of the subtropical gyres. This study used California margin sediments, recovered during Ocean Drilling Program (ODP) Leg 167, as a monitor of gyral circulation in the North Pacific. ODP Leg 167 recovered high accumulation rate records from the Pleistocene and Pliocene and lower-resolution records to examine much of the Neogene interval (Table 1). Although postcruise research has just begun, shipboard measurements identify general trends in the evolution of Pacific climate from the latest Miocene to the Pleistocene. The results presented here highlight one intriguing pattern in California margin regional sedimentation: a relatively expanded middle Pliocene sedimentary section with extremely high $CaCO_3$ mass accumulation rates (MARs). These results suggest that subtropical gyral wind strength was enhanced in the Pliocene, particularly from 2.5 to 3.5 Ma.

[1]Institute of Marine Sciences, University of California, Santa Cruz.
[2]Center for Geophysical Investigation of the Shallow Subsurface, Boise State University, Boise, Idaho.
[3]Division of Earth and Planetary Sciences, Hokkaido University, Sapporo, Japan.
[4]Laboratoire de Geologie, Museum National d'Histoire Naturelle, Paris.
[5]Dipartimento di Geologia, Paleontologia e Geofisica, Universita degli Studi de Padova, Padova, Italy.
[6]Science and Engineering Research Institute, Doshisha University, Tanabe, Japan.
[7]Institut fur Geophysik, Universitat Munchen, Munchen, Germany.
[8]Marine Geology and Geophysics, Rosenstiel School of Marine and Atmospheric Sciences, University of Miami, Miami, Florida.
[9]Geosciences Department, Indiana State University of Pennsylvania, Indiana.
[10]Antartic Research Facilty, Department of Geology, Florida State University, Tallahassee, Florida.
[11]Institute for Geology and Mineralogy, University of Erlangen, Erlangen, Germany.
[12]Fuel Resources Department, Geological Survey of Japan, Tsukuba, Japan.



Paper number 97PA02525
0883-8304/97/97PA-02525$12.00

## 2. California Margin Hydrography

The California Current consists of southward jets concentrated ~250-350 km from the coast at the border of Oregon and California and 300 km from the coast at Point Conception (~35°N) [*Hickey*, 1979; *Lynn and Simpson*, 1987]. Winds along the coast (Figure 1) control seasonal changes, whereas changes in the dynamic topography of the basin-wide North Pacific Gyre control interannual variability in the current strength [*Pares-Sierra and O'Brien*, 1989]. Over much longer climatic cycles monitored by paleoceanographic studies the winds associated with the North Pacific Gyre are expected to have a major impact on the hydrographic features along the California margin. For example, changes in the north Pacific high (strengthening of the wind stress curl adjacent to the California margin) at 18 ka [*Kutzbach*, 1987; *Kutzbach et al.*,1993] enhanced the strength of offshore upwelling [*Ortiz et al.*, 1997].

**Table 1.** Leg 167 Site Information

| Site | Location | Water Depth, m | Basin Sill Depth, m | Sediment Thickness Drilled, mbsf | Age of Oldest Sediment |
|---|---|---|---|---|---|
| 1010 | Pelagic site, near Guadelupe Island | 3465 | | 209 | middle Miocene |
| 1011 | Animal Basin | 2033 | 1600 | 276 | late Miocene |
| 1012 | East Cortez Basin | 1783 | 1415 | 274 | late Miocene |
| 1013 | San Nicholas Basin | 1575 | 1106 | 146 | late Pliocene |
| 1014 | Tanner Basin | 1177 | 1165 | 449 | late Miocene |
| 1015 | Santa Monica Basin | 912 | 737 | 150 | late Pleistocene |
| 1016 | Pelagic site, off Point Conception | 3846 | | 317 | late Miocene |
| 1017 | Santa Lucia Slope | 967 | | 204 | Pleistocene |
| 1018 | Sediment drift, south of Guide Seamount | 2476 | | 426 | late Pliocene |
| 1019 | Eel River Basin | 989 | | 248 | Pleistocene |
| 1020 | Eastern flank, Gorda Ridge | 3050 | | 278 | early Pliocene |
| 1021 | Outer Delgada Fan | 4212 | | 310 | middle Miocene |
| 1022 | Delgada Slope | 1950 | | 388 | early Pliocene |

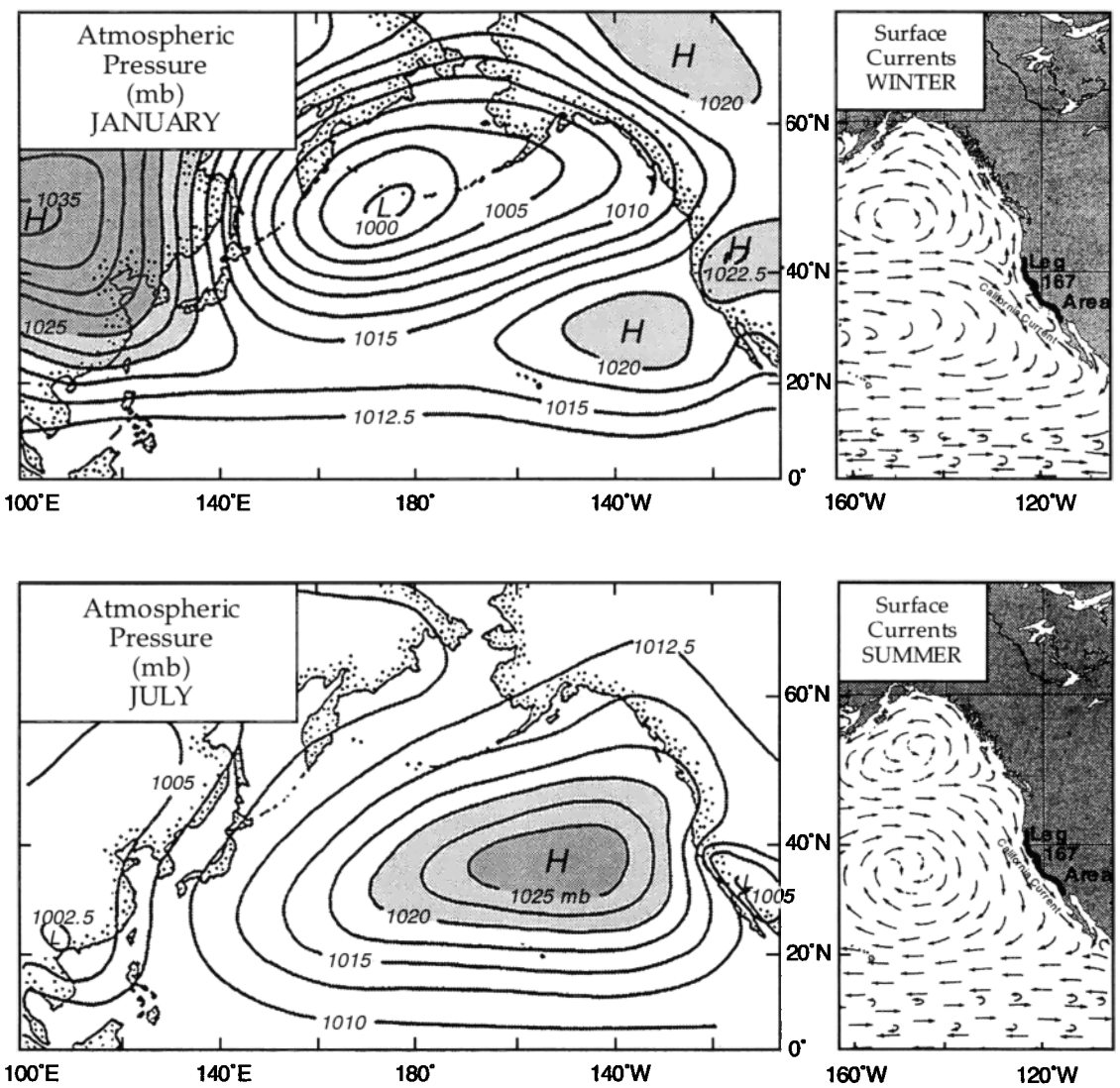


**Figure 1.** Surface atmospheric pressure, winter and summer, from *Huyer* [1983] compared to seasonal changes in northeast Pacific surface currents [*Defense Mapping Agency*, 1989]. Surface winds will approximately parallel atmospheric pressure gradients. Note that seasonal variation in current patterns is driven by northeastern Pacific winds.

Equatorward winds, roughly parallel to the coast, drive Ekman transport of surface waters away from the coast and upwelling of nutrient-rich waters along the coast of California [*Huyer*, 1983]. These winds are seasonal in northern California but blow year-round south of San Francisco. The strongest coastal upwellings occurs between Cape Blanco and San Francisco in the north during the summer, and south of San Diego during the winter [*Huyer*, 1983]. The seasonal cycle of winds and upwelling is a direct result of the annual migration of the North Pacific high-pressure regime [Figure 1; *Huyer*,1983]. Upwelling also occurs offshore if there is sufficient curl to the wind stress, that is if the northerly winds strengthen progressively away from the coast [*Chelton*, 1982; *Chelton et al.*, 1982]. This offshore upwelling is another indication of wind strength, and it can be tracked by its own distinct biological community. Paleoceanographic data of the history of upwelling along coastal and offshore California can be used to infer the latitudinal position and strength of the North Pacific high as climate changes.

Site selection for the Leg 167 program (Table 1) was designed to monitor both the surface water expression of the California Current, and the deep and intermediate water masses of the northeast Pacific. The sites used in this study are those with complete sections from the late Pleistocene to at least the middle Pliocene. These sites are not situated in the present-day coastal upwelling zone; rather, they are located further offshore and should record nutrient supply to surface waters through offshore upwelling.

## 3. Leg 167 Results

### 3.1. Calculation of $CaCO_3$ MAR and $C_{org}$ MAR

Shipboard age models, weight percent carbonate (wt % $CaCO_3$), weight percent organic carbon (wt % $C_{org}$), and bulk density measurements [*Lyle et al.*, 1997] were compiled to calculate $CaCO_3$ MAR and $C_{org}$ MAR. The wt % $CaCO_3$ was calculated from inorganic carbon (IC) measurements made by coulometry with a precision of <1% (1σ standard deviation of means of multiple determinations of a pure carbonate standard). Total organic carbon (precision of 1-2%) was calculated by the difference between total carbon (measured using the shipboard Nitrogen-Carbon-Sulfur analyzer) and IC (see Explanatory Notes by *Lyle et al.* [1997]). At each site, gamma ray attenuation porosity evalator (GRAPE), magnetic susceptibility, and reflectance percentage data [*Lyle et al.*, 1997] were used to correlate among holes and to build a composite stratigraphic section. All measurements were then placed on the meters composite depth (mcd) scale (see Explanatory Notes by *Lyle et al.* [1997]) so that measurements from adjacent holes at a site could be placed in stratigraphic sequence relative to each other.

Age models (Table 2) were constructed using paleomagnetic boundaries on the timescale of *Cande and Kent* [1995]. In sections where paleomagnetic boundaries could not be resolved using the shipboard magnetometer, nannofossil, diatom, and radiolaria biostratigraphic data, all calibrated to the *Cande and Kent* [1995] timescale, were used. Although these shipboard biostratigraphic data are based only on core-catcher samples spaced ~10 m apart, the actual error in the depth of most biostratigraphic data was reduced by combining data from multiple holes to further constrain the depth of an event.

On the basis of the shipboard age models all data were binned into 0.5 m.y. intervals and averaged. $CaCO_3$ MAR and $C_{org}$ MAR were calculated from the average sedimentation rate, average bulk density, average wt % $CaCO_3$, and average wt % $C_{org}$ of each 0.5 m.y. interval (Table 2,and Figure 2). Although there are significant regional differences in the Plio-Pleistocene history of $CaCO_3$ MAR along the California margin, most sites have a distinct peak in accumulation rate occurring in the middle Pliocene (3.5-2.5 Ma). The borderland sites have expanded maxima compared to the other sites from Leg 167 (1011 maximum is from 4.5 to 2.0 Ma; 1012 maximum is from 4.0 to 0.5 Ma). The peak in $CaCO_3$ MAR at Site 1010 is slightly older than the other sites (4.0-3.0 Ma). The maximum $CaCO_3$ MAR at the northern sites (1020 and 1021) also occurs slightly before (3.5-3.0 Ma) the maximum at the southern sites (1014, 1016,and 1018) (3.0-2.5 Ma). Large regional hydrographic differences probably contribute to the intersite differences in the timing and duration of the middle-Pliocene $CaCO_3$ MAR (see section 4).

While $CaCO_3$ MAR records are used in this study to assess offshore upwelling, $C_{org}$ MAR are not thought to reflect offshore upwelling strength [*Lyle et al.*, 1992]. Therefore $C_{org}$ MAR records are not expected to mirror $CaCO_3$ MAR,and are presented (Figure 2) and discussed in this study (section 4.1below) only for the purpose of assessing dissolution due to organic matter remineralization in shallow sites above the lysocline.

Diachrony of biostratigraphic data probably does not affect the calculations presented here because MAR estimates are averaged over 0.5 m.y. intervals and because biostratigraphic data are chosen on the basis of whether there is agreement with other microfossil groups when available. We tested the sensitivity of MAR calculations for sites whose age models rely on biostratigraphic age data. For all sites using biostratigraphic age data, except Site 1018, a 100,000 year error in datum age, or a 10 m error in datum depth, resulted in a change of <10% in $CaCO_3$ MAR and $C_{org}$ MAR. For both the large- and small- amplitude trends in $CaCO_3$ MAR and $C_{org}$ MAR, such as at Site 1014 and Site 1011, respectively, the age of more than one biostratigraphic event needed to be changed by over 500,000 years to significantly change the structure and timing of the Pliocene-Pleistocene trends. Site 1018 is the only site whose $CaCO_3$ MAR and $C_{org}$ MAR records are significantly dependent on one age datum. For example, if the oldest datum used in the 1018 age model were assumed to be 100,000 years older, the middle-Pliocene trend from higher to lower $CaCO_3$ MAR would be greatly diminished.

While the history of $CaCO_3$ MAR at sites drilled on Leg 167 can be characterized by relatively high rates during the middle Pliocene at all sites, there are large intersite differences in the absolute rates. In the late Pleistocene, the highest absolute rates occur at the California Borderland sites where $CaCO_3$ MAR is above 1 g/ $cm^{-2}$/ $kyr^{-1}$(Fig 3a). Although $CaCO_3$ MARs are higher than present over the entire California margin region in the middle Pliocene (Figures 3b -3d), they are always highest in the California Borderland and some of the southern pelagic sites. $CaCO_3$ MARs are > 2 g/ $cm^{-2}$/ $kyr^{-1}$ and as high as 11.5 g/ $cm^{-2}$/ $kyr^{-1}$ at Tanner Basin, while at the

**Table 2.** Age Model Control Points and Measured Parameters used in $CaCO_3$ Mass Accumulation Rate (MAR) and $C_{org}$ MAR Calculations

| Age Model Data | | | Binned Data for Each Age Interval | | | | | | | |
|---|---|---|---|---|---|---|---|---|---|---|
| Event * | Age, Ma | Depth, mcd | Age Interval, Ma † | Depth, mcd ‡ | Sed. Rate, mcd myr$^{-1}$ | Dry Bulk Density, g cm$^{-3}$ | $CaCO_3$, % | $CaCO_3$ MAR, g cm$^{-2}$ kyr$^{-1}$ | Organic C, % | Organic C MAR, g cm$^{-2}$ kyr$^{-1}$ |
| | | | | | *Site 1010* | | | | | |
| Brunhes (o) | 0.78 | 9.46 | 0.00 | 0.00 | 12.1 | 0.66 | 1.33 | 0.01 | 0.35 | 0.003 |
| Jaramillo (t) | 0.99 | 12.16 | 0.50 | 6.06 | 12.3 | 0.65 | 2.54 | 0.02 | 0.19 | 0.002 |
| Olduvai (t) | 1.77 | 17.40 | 1.00 | 12.23 | 6.7 | 0.61 | 9.00 | 0.04 | 0.40 | 0.002 |
| Reunion (t) | 2.42 | 19.50 | 1.50 | 15.59 | 5.1 | 0.72 | 10.50 | 0.04 | 0.33 | 0.001 |
| Gauss (t) | 2.58 | 22.00 | 2.00 | 18.14 | 5.2 | 0.62 | 2.58 | 0.01 | 0.30 | 0.001 |
| C2An.2n (t) | 3.11 | 26.40 | 2.50 | 20.74 | 9.5 | 0.68 | 16.23 | 0.10 | 0.25 | 0.002 |
| C2An.3n (t) | 3.33 | 33.86 | 3.00 | 25.49 | 22.5 | 0.78 | 25.81 | 0.45 | 0.23 | 0.004 |
| Cochiti (t) | 4.18 | 48.31 | 3.50 | 36.75 | 17.0 | 0.86 | 33.45 | 0.49 | 0.08 | 0.001 |
| Nunivak (t) | 4.48 | 52.11 | 4.00 | 45.25 | 14.1 | 0.83 | 10.70 | 0.12 | 0.15 | 0.002 |
| Sidufjall (t) | 4.80 | 55.06 | 4.50 | 52.29 | 10.6 | 0.66 | 1.21 | 0.01 | 0.24 | 0.002 |
| Thvera (t) | 4.98 | 57.36 | 5.00 | 57.59 | 12.6 | 0.64 | 26.58 | 0.21 | 0.19 | 0.001 |
| C3An.1n (t) | 5.89 | 67.83 | 6.00 | 70.18 | 13.4 | 0.68 | 18.04 | 0.16 | 0.24 | 0.002 |
| C3An.2n (t) | 6.27 | 76.13 | 7.00 | 83.57 | 10.6 | 0.64 | 14.55 | 0.10 | 0.23 | 0.002 |
| C3Bn (t) | 6.94 | 82.88 | 8.00 | 94.16 | 10.6 | 0.68 | 20.86 | 0.15 | 0.28 | 0.002 |
| T *D. hamatus* | 9.49 | 109.93 | 9.00 | 104.74 | 19.0 | 0.69 | 17.60 | 0.23 | 0.18 | 0.002 |
| B *D. hamatus* | 10.50 | 137.30 | 10.00 | 123.75 | 22.3 | 0.70 | 20.47 | 0.32 | 0.13 | 0.002 |
| T *C. premacintyrei* | 12.22 | 167.45 | 11.00 | 146.06 | 17.5 | 0.62 | 30.98 | 0.34 | 0.25 | 0.003 |
| T *S. heteromorphus* | 13.60 | 203.65 | 12.00 | 163.59 | 24.3 | 0.58 | 37.11 | 0.52 | 0.24 | 0.003 |
| | | | 13.00 | 187.91 | 21.7 | 0.74 | 44.63 | 0.72 | 0.18 | 0.003 |
| | | | 13.60 | 203.65 | | | | | | |
| | | | | | *Site 1011* | | | | | |
| T *P. lacunosa* | 0.46 | 20.90 | 0.00 | 0.00 | 44.6 | 0.78 | 9.34 | 0.32 | 1.32 | 0.046 |
| T *D. pentaradiatus* | 2.50 | 92.67 | 0.50 | 22.30 | 35.2 | 0.87 | 15.73 | 0.48 | 1.20 | 0.037 |
| T *D. quinqueramus* | 5.56 | 167.04 | 1.00 | 39.90 | 35.2 | 0.94 | 10.88 | 0.36 | 1.45 | 0.048 |
| CT *D. hustedtii* | 8.60 | 252.44 | 1.50 | 57.49 | 35.2 | 0.94 | 14.46 | 0.48 | 1.90 | 0.063 |
| T *D. dimorpha* | 9.16 | 271.69 | 2.00 | 75.08 | 35.2 | 0.95 | 29.89 | 1.00 | 1.67 | 0.056 |
| | | | 2.50 | 92.67 | 24.3 | 0.99 | 28.08 | 0.68 | 1.52 | 0.037 |
| | | | 3.00 | 104.82 | 24.3 | 1.04 | 38.65 | 0.97 | 1.11 | 0.028 |
| | | | 3.50 | 116.98 | 24.3 | 1.03 | 29.53 | 0.74 | 1.15 | 0.029 |
| | | | 4.00 | 129.13 | 24.3 | 1.07 | 47.13 | 1.23 | 1.36 | 0.035 |
| | | | 4.50 | 141.28 | 24.3 | 1.16 | 25.18 | 0.71 | 1.73 | 0.049 |
| | | | 5.00 | 153.43 | 26.0 | 1.12 | 21.39 | 0.62 | 1.57 | 0.046 |
| | | | 6.00 | 179.40 | 28.1 | 0.93 | 27.01 | 0.71 | 1.97 | 0.052 |
| | | | 7.00 | 207.49 | 28.1 | 0.93 | 12.61 | 0.33 | 1.24 | 0.032 |
| | | | 8.00 | 235.58 | 30.6 | 0.80 | 16.25 | 0.40 | 2.26 | 0.055 |
| | | | 9.16 | 271.69 | | | | | | |
| | | | | | *Site 1012* | | | | | |
| T *P.lacunosa* | 0.46 | 36.90 | 0.00 | 0.00 | 80.0 | 0.76 | 22.51 | 1.38 | 2.64 | 0.162 |
| Brunhes (o) | 0.78 | 61.85 | 0.50 | 40.02 | 73.1 | 0.88 | 31.90 | 2.05 | 2.41 | 0.155 |
| Jaramillo (t) | 0.99 | 75.95 | 1.00 | 76.57 | 62.3 | 0.94 | 39.12 | 2.30 | 2.69 | 0.158 |
| Olduvai (t) | 1.77 | 124.57 | 1.50 | 107.74 | 72.0 | 0.95 | 42.53 | 2.90 | 3.19 | 0.217 |
| T *D. brouweri* | 1.96 | 141.61 | 2.00 | 143.74 | 53.3 | 0.95 | 51.06 | 2.59 | 3.05 | 0.155 |
| T *D. pentaradiatus* | 2.50 | 170.41 | 2.50 | 170.41 | 64.5 | 0.97 | 46.28 | 2.88 | 2.35 | 0.146 |
| T *R. pseudoummbilicus* | 3.79 | 253.56 | 3.00 | 202.64 | 64.5 | 0.95 | 48.94 | 3.01 | 1.97 | 0.121 |
| B *C. rugosus* | 5.07 | 277.11 | 3.50 | 234.87 | 45.1 | 0.95 | 52.35 | 2.24 | 2.43 | 0.104 |
| | | | 4.00 | 257.42 | 18.4 | 0.99 | 54.43 | 0.99 | 1.98 | 0.036 |
| | | | 4.50 | 266.62 | 18.4 | 1.04 | 48.87 | 0.93 | 2.13 | 0.041 |
| | | | 5.07 | 277.11 | | | | | | |
| | | | | | *Site 1013* | | | | | |
| T *P.lacunosa* | 0.46 | 35.66 | 0.00 | 0.00 | 76.6 | 0.78 | 16.23 | 0.97 | 4.36 | 0.260 |
| Brunhes (o) | 0.78 | 56.64 | 0.50 | 38.28 | 56.1 | 0.91 | 24.06 | 1.22 | 3.97 | 0.202 |
| Jaramillo (t) | 0.99 | 65.97 | 1.00 | 66.31 | 33.9 | 0.91 | 26.61 | 0.83 | 3.49 | 0.108 |
| Olduvai (t) | 1.77 | 92.44 | 1.50 | 83.28 | 44.1 | 0.90 | 31.56 | 1.25 | 4.51 | 0.179 |
| T *D. tamalis* | 2.76 | 148.00 | 2.00 | 105.35 | 56.1 | 0.95 | 41.83 | 2.23 | 3.46 | 0.185 |
| | | | 2.50 | 133.41 | 56.1 | 0.97 | 43.74 | 2.39 | 2.97 | 0.162 |
| | | | 2.76 | 148.00 | | | | | | |

**Table 2.** (Continued)

| Age Model Data | | | Binned Data for Each Age Interval | | | | | | | |
|---|---|---|---|---|---|---|---|---|---|---|
| Event * | Age, Ma | Depth, mcd | Age Interval, Ma † | Depth, mcd ‡ | Sed. Rate, mcd myr$^{-1}$ | Dry Bulk Density, g cm$^{-3}$ | $CaCO_3$ % | $CaCO_3$ MAR, g cm$^{-2}$ kyr$^{-1}$ | Organic C, % | Organic C MAR, g cm$^{-2}$ kyr$^{-1}$ |
| | | | | | *Site 1014* | | | | | |
| T *P.lacunosa* | 0.46 | 37.79 | 0.00 | 0.00 | 82.5 | 0.72 | 30.57 | 1.81 | 4.74 | 0.281 |
| Brunhes (o) | 0.78 | 65.66 | 0.50 | 41.27 | 81.8 | 0.82 | 42.44 | 2.85 | 4.88 | 0.328 |
| Jaramillo (t) | 0.99 | 81.58 | 1.00 | 82.15 | 56.5 | 0.87 | 43.89 | 2.17 | 4.70 | 0.233 |
| B *G. oceanica* | 1.69 | 121.16 | 1.50 | 110.42 | 83.3 | 0.81 | 47.29 | 3.20 | 6.54 | 0.443 |
| T *D. surculus* | 2.61 | 212.86 | 2.00 | 152.06 | 99.7 | 0.92 | 57.18 | 5.23 | 4.09 | 0.374 |
| T *D. tamalis* | 2.76 | 254.80 | 2.50 | 201.90 | 213.8 | 0.95 | 56.74 | 11.53 | 4.26 | 0.866 |
| B *L. neoheteroporos* | 3.06 | 322.30 | 3.00 | 308.80 | 50.6 | 0.97 | 60.62 | 2.98 | 4.09 | 0.201 |
| B *Ceratolithus* spp. | 5.03 | 375.00 | 3.50 | 334.10 | 26.8 | 1.01 | 58.10 | 1.58 | 4.20 | 0.114 |
| | | | 4.00 | 347.51 | 26.8 | 1.03 | 49.31 | 1.36 | 4.67 | 0.129 |
| | | | 4.50 | 360.92 | 26.8 | 0.96 | 62.18 | 1.60 | 5.50 | 0.142 |
| | | | 5.03 | 375.00 | | | | | | |
| | | | | | *Site 1016* | | | | | |
| T *P.lacunosa* | 0.46 | 24.52 | 0.00 | 0.00 | 52.0 | 0.65 | 3.87 | 0.13 | 1.05 | 0.035 |
| T *R. matuyamai* | 0.98 | 43.37 | 0.50 | 25.99 | 36.6 | 0.73 | 7.60 | 0.20 | 1.07 | 0.029 |
| B *G. oceanica* | 1.69 | 69.77 | 1.00 | 44.29 | 36.9 | 0.73 | 6.90 | 0.19 | 1.18 | 0.032 |
| T *D. brouweri* | 1.96 | 84.77 | 1.50 | 62.75 | 49.9 | 0.71 | 14.58 | 0.51 | 1.55 | 0.055 |
| T *T. convexa* | 2.40 | 117.34 | 2.00 | 87.73 | 71.2 | 0.70 | 27.90 | 1.38 | 1.04 | 0.052 |
| T *A. pliocenica* | 3.36 | 174.61 | 2.50 | 123.31 | 59.7 | 0.82 | 42.82 | 2.10 | 0.49 | 0.024 |
| T *R. pseudoummbilicus* | 3.79 | 178.24 | 3.00 | 153.13 | 45.3 | 0.90 | 42.54 | 1.74 | 0.77 | 0.032 |
| B *Ceratolithus* spp. | 5.03 | 192.66 | 3.50 | 175.79 | 9.8 | 0.92 | 40.57 | 0.36 | 0.71 | 0.006 |
| T *D. splendens* | 5.90 | 221.07 | 4.00 | 180.69 | 11.7 | 0.82 | 18.54 | 0.18 | 0.71 | 0.007 |
| T *L. n nipponica* | 6.25 | 246.20 | 4.50 | 186.53 | 11.7 | 0.82 | 11.87 | 0.11 | 0.97 | 0.009 |
| | | | 5.00 | 192.37 | 35.9 | 0.66 | 15.59 | 0.37 | 0.82 | 0.020 |
| | | | 6.00 | 228.25 | 71.8 | 0.53 | 6.84 | 0.26 | 0.84 | 0.032 |
| | | | 6.25 | 246.20 | | | | | | |
| | | | | | *Site 1017* | | | | | |
| T *P.lacunosa* | 0.46 | 97.44 | 0.00 | 0.00 | 204.3 | 1.16 | 7.12 | 1.69 | 1.45 | 0.344 |
| T large *Gephyrocapsa* spp. | 1.24 | 189.09 | 0.50 | 102.14 | 117.5 | 1.27 | 9.76 | 1.45 | 1.60 | 0.238 |
| | | | 1.00 | 160.89 | 117.5 | 1.25 | 11.69 | 1.72 | 2.41 | 0.355 |
| | | | 1.24 | 189.09 | | | | | | |
| | | | | | *Site 1018* | | | | | |
| T *P.lacunosa* | 0.46 | 91.33 | 0.00 | 0.00 | 192.6 | 0.84 | 3.15 | 0.51 | 1.21 | 0.197 |
| T *R. matuyamai* | 0.98 | 155.30 | 0.50 | 96.29 | 123.1 | 0.91 | 3.30 | 0.37 | 1.49 | 0.167 |
| B *G. oceanica* | 1 69 | 227.46 | 1.00 | 157.82 | 100.9 | 0.95 | 4.17 | 0.40 | 1.30 | 0.124 |
| T *T. convexa* | 2.40 | 315.99 | 1.50 | 208.28 | 115.7 | 0.92 | 2.57 | 0.27 | 1.51 | 0.160 |
| T *D. surculus* | 2.61 | 344.84 | 2.00 | 266.11 | 127.2 | 0.92 | 4.71 | 0.55 | 1.34 | 0.157 |
| T *D. tamalis* | 2.76 | 373.89 | 2.50 | 329.73 | 103.8 | 0.99 | 4.83 | 0.49 | 1.15 | 0.118 |
| T *A. pliocenica* | 3.36 | 393.19 | 3.00 | 381.61 | 55.9 | 1.05 | 13.55 | 0.80 | 1.18 | 0.069 |
| | | | 3.36 | 393.19 | | | | | | |
| | | | | | *Site 1019* | | | | | |
| T *P.lacunosa* | 0.46 | 55.94 | 0.00 | 0.00 | 151.7 | 1.13 | 4.20 | 0.72 | 1.02 | 0.175 |
| Evol. boundary betw. *L. neoheteroporos* and *L. nigriniae* | 0.85 | 250.19 | 0.50 | 75.86 | 498.1 | 1.25 | 3.38 | 2.10 | 1.03 | 0.643 |
| | | | 0.85 | 250.19 | | | | | | |
| | | | | | *Site 1020* | | | | | |
| T *P.lacunosa* | 0.46 | 51.30 | 0.00 | 0.00 | 111.0 | 0.79 | 5.14 | 0.45 | 0.76 | 0.067 |
| Brunhes (o) | 0.78 | 84.83 | 0.50 | 55.49 | 92.4 | 0.86 | 3.94 | 0.31 | 0.78 | 0.062 |
| Jaramillo (t) | 0.99 | 100.68 | 1.00 | 101.70 | 93.6 | 0.89 | 3.79 | 0.31 | 0.78 | 0.065 |
| Jaramillo (o) | 1.07 | 108.81 | 1.50 | 148.48 | 91.9 | 0.90 | 3.23 | 0.27 | 0.79 | 0.065 |
| T large *Gephyrocapsa* spp. | 1.24 | 125.01 | 2.00 | 194.44 | 92.6 | 0.83 | 7.75 | 0.59 | 0.86 | 0.066 |
| B large *Gephyrocapsa* spp. | 1.44 | 144.69 | 2.50 | 240.74 | 31.4 | 0.96 | 27.41 | 0.83 | 0.60 | 0.018 |
| B *G. oceanica* | 1.69 | 160.48 | 3.00 | 256.43 | 41.3 | 1.07 | 37.70 | 1.67 | 0.46 | 0.020 |
| T *T. convexa* | 2.40 | 238.27 | 3.50 | 277.09 | 41.3 | 1.19 | 12.81 | 0.63 | 0.66 | 0.033 |
| B *C. davisiana* | 2.80 | 248.17 | 3.79 | 289.07 | | | | | | |
| T *R. pseudoummbilicus* | 3.79 | 289.07 | | | | | | | | |
| | | | | | *Site 1021* | | | | | |
| Brunhes (o) | 0.78 | 27.16 | 0.00 | 0.00 | 34.8 | 0.62 | 4.29 | 0.09 | 0.56 | 0.012 |
| Jaramillo (t) | 0.99 | 33.23 | 0.50 | 17.41 | 32.2 | 0.69 | 2.30 | 0.05 | 0.48 | 0.011 |

**Table 2.** (Continued)

| Age Model Data | | | Binned Data for Each Age Interval | | | | | | | |
|---|---|---|---|---|---|---|---|---|---|---|
| Event * | Age, Ma | Depth, mcd | Age Interval, Ma † | Depth, mcd ‡ | Sed. Rate, mcd myr$^{-1}$ | Dry Bulk Density, g cm$^{-3}$ | $CaCO_3$ % | $CaCO_3$ MAR, g cm$^{-2}$ kyr$^{-1}$ | Organic C, % | Organic C MAR, g cm$^{-2}$ kyr$^{-1}$ |
| Olduvai (t) | 1.77 | 55.33 | 1.00 | 33.51 | 28.3 | 0.70 | 3.21 | 0.06 | 0.39 | 0.008 |
| Reunion (t) | 2.14 | 67.54 | 1.50 | 47.68 | 30.5 | 0.68 | 3.62 | 0.07 | 0.46 | 0.009 |
| Gauss (t) | 2.58 | 86.03 | 2.00 | 62.92 | 39.4 | 0.70 | 11.55 | 0.32 | 0.51 | 0.014 |
| C2An.2n (t) | 3.11 | 107.16 | 2.50 | 82.63 | 40.3 | 0.69 | 15.04 | 0.42 | 0.34 | 0.009 |
| C2An.3n (t) | 3.33 | 113.14 | 3.00 | 102.76 | 32.5 | 0.79 | 34.61 | 0.89 | 0.28 | 0.007 |
| Gauss (o) | 3.58 | 121.80 | 3.50 | 119.03 | 26.1 | 0.71 | 5.46 | 0.10 | 0.40 | 0.007 |
| Cochiti (t) | 4.18 | 136.50 | 4.00 | 132.09 | 23.7 | 0.74 | 2.27 | 0.04 | 0.41 | 0.007 |
| Nunivak (t) | 4.48 | 143.15 | 4.50 | 143.93 | 35.9 | 0.68 | 1.62 | 0.04 | 0.45 | 0.011 |
| Sidufjall (t) | 4.80 | 155.67 | 5.00 | 161.86 | 26.8 | 0.64 | 3.88 | 0.07 | 0.39 | 0.007 |
| Thvera (o) | 5.23 | 168.99 | 6.00 | 188.71 | 25.6 | 0.72 | 4.89 | 0.09 | 0.33 | 0.006 |
| T *T. schraderi* | 7.40 | 224.56 | 7.00 | 214.32 | 24.3 | 0.62 | 6.47 | 0.10 | 0.32 | 0.005 |
| B *M. convallis* | 9.46 | 272.66 | 8.00 | 238.57 | 23.3 | 0.63 | 26.36 | 0.39 | 0.22 | 0.003 |
| T *C. japonica* | 10.05 | 291.91 | 9.00 | 261.92 | 28.4 | 0.64 | 14.53 | 0.26 | 0.13 | 0.002 |
| T *C. cornuta* | 11.82 | 311.11 | 10.00 | 290.28 | 12.0 | 0.59 | 3.39 | 0.02 | 0.11 | 0.001 |
| | | | 11.00 | 302.24 | 10.8 | 0.54 | 0.86 | 0.01 | 0.10 | 0.001 |
| | | | 11.82 | 311.11 | | | | | | |

* For biostratigraphic data, T is top and B is base. For paleomagnetic boundaries, o is onset and t is termination.
† Age of beginning of bin. The age of end of bin is on subsequent row.
‡ The mcd is meters composite depth. See text and *Lyle et al.* [1997], for explanation.

northern sites (e.g., 1020), $CaCO_3$ MARs are only >1 g/ cm$^{-2}$/ kyr$^{-1}$ for the interval between 3.5 and 3.0 Ma.

### 3.2. Pacific Comparison

The pattern of $CaCO_3$ MAR in the California margin is notably different from that in the tropical Pacific (Figure 4). Neogene records of $CaCO_3$ MAR in the eastern tropical Pacific (e.g., Site 846) [*Farrell et al.*, 1995], the central tropical Pacific (e.g. Site 574) [*Farrell et al.*, 1995], and in the western tropical Pacific (Site 806) [*Berger et al.*, 1991] have highest values in the late Miocene to early Pliocene. The tropical Pacific trends resemble Indian Ocean trends [*Peterson et al.*, 1992], suggesting that the shift from higher to lower $CaCO_3$ MAR in the early Pliocene is actually an Indo-Pacific pattern. The lowest values in the tropical Pacific occur in the middle Pliocene when $CaCO_3$ MAR was highest in the region of the California margin. Absolute fluxes are also different between the two regions with "low" $CaCO_3$ MAR values in the tropical Pacific of 1.0-1.5 g/ cm$^{-2}$/ kyr$^{-1}$ being higher than most of the highest values in the California margin with the notable exception of Tanner Basin (1014) and San Nicholas Basin (1012). Tanner Basin has extraordinarily high $CaCO_3$ MAR values, in excess of 11 g/ cm$^{-2}$/ kyr$^{-1}$, compared to maximum values of 0.5-3.0 g/ cm$^{-2}$/ kyr$^{-1}$ in the rest of the California margin and maximum values of 3.0-3.5 g/ cm$^{-2}$/ kyr$^{-1}$ at tropical Pacific Site 846.

The timing of changes in $CaCO_3$ MAR in the California margin sediments is most similar to that in the North Pacific, represented here by Site 882 [*Haug et al.*, 1995], with the exception of the timing of the end of the event (Figure 4). In the Leg 167 sediments, excluding Site 1010 which clearly has a different history of $CaCO_3$ MAR, the middle-Pliocene high $CaCO_3$ MAR event ends at ~2.0 Ma. There may be a two-step decrease at some of the sites: one step between 2.5 and 3.0 Ma and another between 1.5 and 2.0 Ma. In contrast, in the North Pacific the high $CaCO_3$ MAR event has a dramatic and clear termination between 2.5 and 3.0 Ma. As described earlier, the timing of the onset and peak of the middle-Pliocene high $CaCO_3$ MAR event among the California margin sites is also variable. The onset and peak of the event at North Pacific Site 882 is most similar to those at the northern sites of the California margin (Figures 2 and 4).

## 4. Discussion

### 4.1. Dissolution Versus Production

Some of the sites from Leg 167 are deep enough to be affected by changes in the depth of the lysocline. In the Pleistocene, sediments as shallow as 2700 m are clearly subject to $CaCO_3$ dissolution, particularly in the interglacial periods [*Karlin et al.*, 1992; *Lyle et al.*, 1992]. However, with the exception of Site 1010, the timing of the mid-Pliocene $CaCO_3$ MAR peak at the deep sites is the same as at some shallow sites (e.g., Site 1014 at 1177 m) where dissolution is unlikely to be the primary cause of $CaCO_3$ MAR fluctuations, unless driven by organic remineralization as discussed below.

The pattern of $CaCO_3$ MAR changes on the California margin is notably different from that in the tropical Pacific. A dramatic decrease in $CaCO_3$ MAR in the equatorial Pacific (e.g., Site 846 in Figure 4), related to the termination of a "biogenic bloom" between 6 and 4 Ma [*Farrell et al.*, 1995], is not observed on the California margin. The most pronounced fluctuation in the carbonate critical depth (CCrD, depth where sediments contain 10% $CaCO_3$) in the tropical Pacific during the Pliocene, interpreted from deep cores (>4000 m water depth) [*Farrell and Prell*, 1991; *Farrell et al.*, 1995], occurs between 3 and 2 Ma when the CCrD deepened. A deeper Pacific

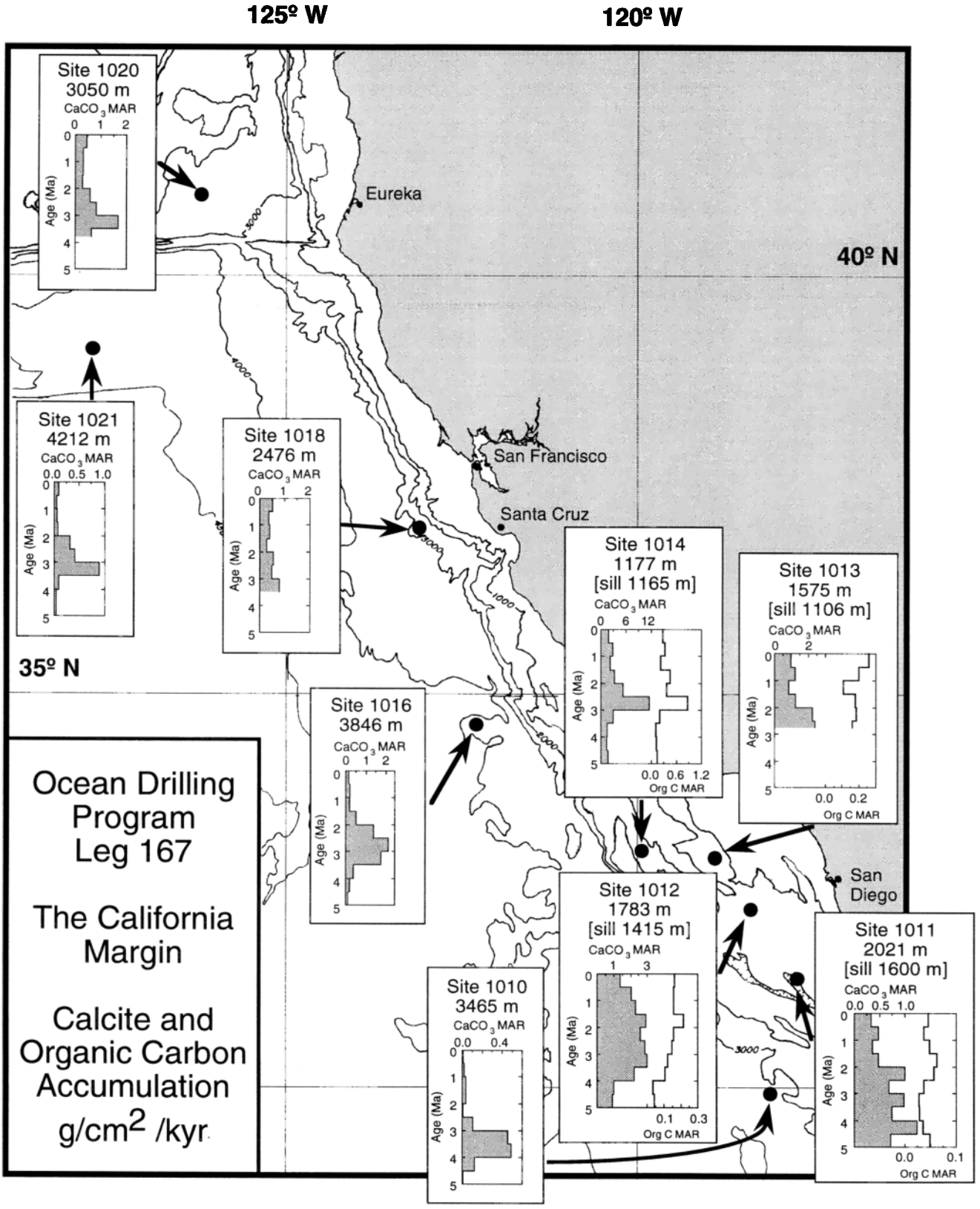


**Figure 2.** Map of $CaCO_3$ mass accumulation rate (MAR) for all Leg 167 sites where Pliocene-Pleistocene sediments were recovered. Organic carbon MAR records for shallow sites (<2000 m) are also shown.

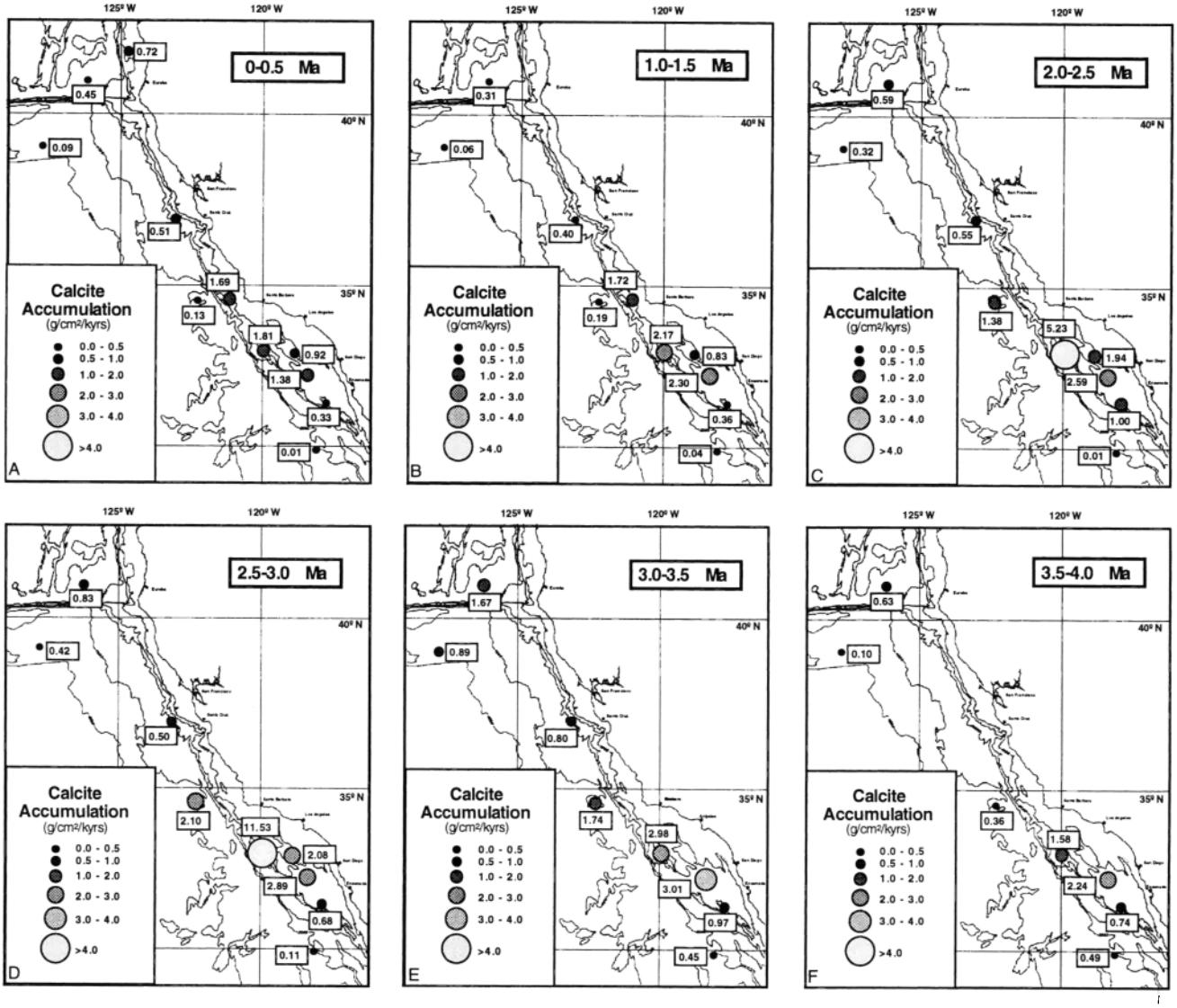


**Figure 3.** Map and $CaCO_3$ MAR for six 0.5 m.y. time periods. Note that the highest $CaCO_3$ MAR values are always in the region of the Southern California Borderlands where year-round offshore upwelling occurs today.

lysocline depth (assuming that the lysocline depth is tracked by the CCrD in the central tropical Pacific) between 3 and 2 Ma may have produced enhanced $CaCO_3$ MARs at the deep California margin sites (1010, 1016, 1018, 1020, and 1021), but it could not have influenced the shallower sites. The timing of the onset of the $CaCO_3$ MAR peak on the California margin (~ 3.5 Ma) predates the preservation event observed in the tropical Pacific.

Both the intersite agreement in first-order $CaCO_3$ MAR trends between shallow and deep sites along the California margin and the partial discordance with the known history of lysocline depth changes in the open Pacific [*Berger et al.*, 1991; *Farrell and Prell*, 1991; *Farrell et al.*, 1995] suggest that the first-order middle Pliocene $CaCO_3$ MAR peak in the region of the California margin is most likely due to enhanced $CaCO_3$ production. However, before discussing the implications of enhanced $CaCO_3$ production along the California margin, alternative explanations involving the influences of dissolution at the shallow sites should be considered.

To invoke dissolution as the main control defining the middle Pliocene $CaCO_3$ MAR peak at the shallow sites requires consideration of dissolution above the lysocline due to organic matter degradation within sediments [e.g., *Emerson and Bender*, 1981; *Archer*, 1991]. For example, reduced dissolution due to a lower ratio of organic carbon to calcite ($C_{org}$:$CaCO_3$) rain rate could explain the observed high $CaCO_3$ MAR during the middle Pliocene. A study of California Borderland basins demonstrates that the organic carbon burial rate is strongly correlated to the organic carbon rain rate [*Jahnke*, 1990]; changes in availability of oxygen within sediments due to bottom water oxygen concentrations, extent of oxic mineralization, and sediment mixing do not significantly influence organic carbon burial rates in these basins. Therefore, if the records of $CaCO_3$ MAR were related to changes in dissolution within the sediment,a relatively low

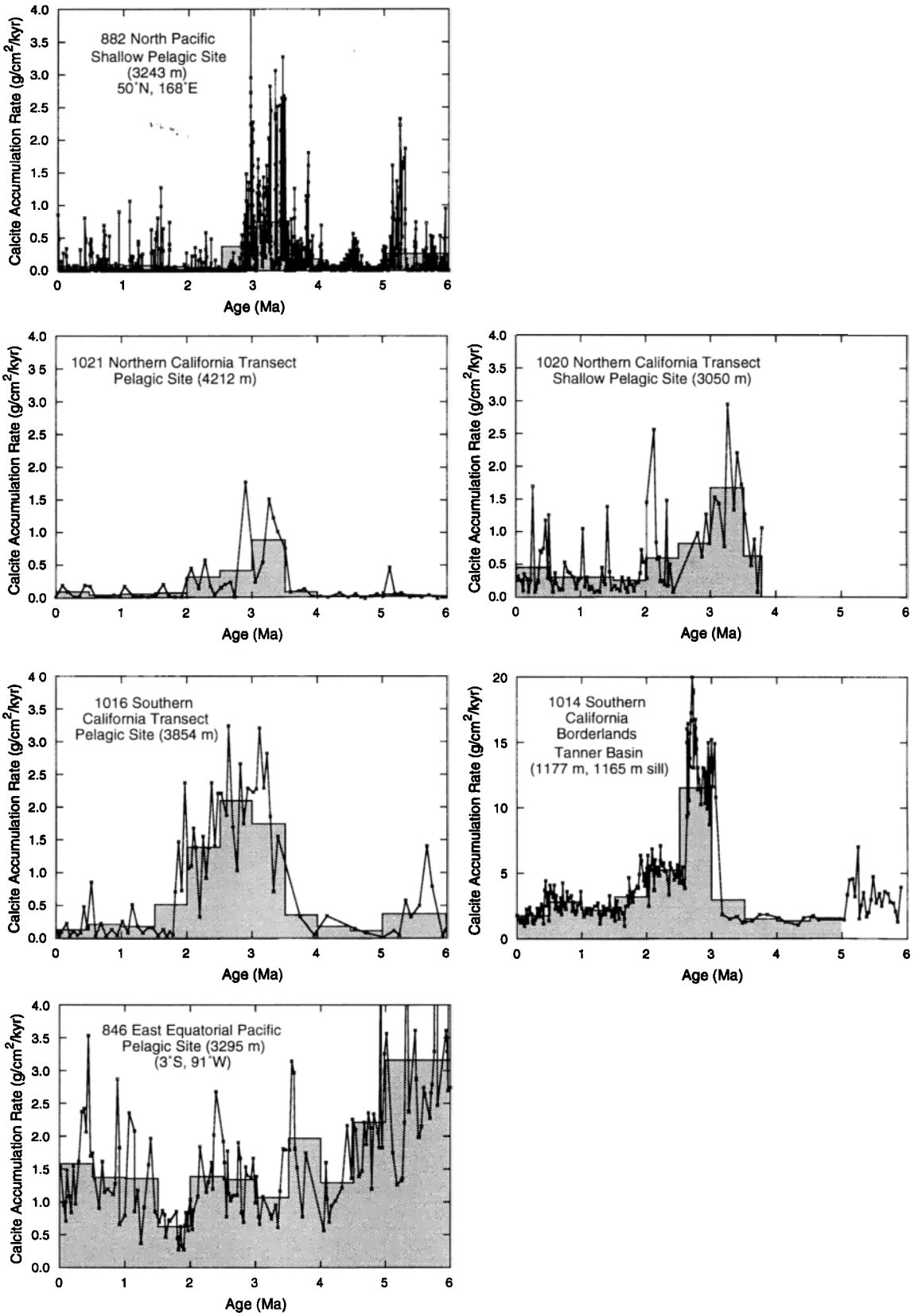


**Figure 4.** $CaCO_3$ MAR records from a North Pacific site, four sites from the California margin, and a tropical Pacific site. Age models for Sites 882 and 846 data have been adjusted to be consistent with the *Cande and Kent* [1995] timescale so they can be accurately compared to the ODP Leg 167 sites. The small squares connected by a solid line show the actual data (unbinned). The shaded area curve shows results from binning the original data into 0.5 m.y. intervals.

$C_{org}$ MAR, reflecting a lower $C_{org}$ rain rate, would be expected during intervals of relatively high $CaCO_3$ MAR. Clearly, this is not the case in the records from the California margin (Figure 2). Only 1011 has slightly lower $C_{org}$ MAR during some intervals when $CaCO_3$ MAR is high. Furthermore, for changes in the $C_{org}$: $CaCO_3$ rain rate to effectively change the extent of $CaCO_3$ dissolution required much larger changes in $C_{org}$ rain rate, as reflected by the $C_{org}$ MAR record, are than are observed; a doubling of the $C_{org}$ rain rate would change the preservation of $CaCO_3$ by 0-30% [*Emerson and Bender*, 1981]. Thus it appears that a change in the $C_{org}$ rain rate alone could not explain the degree of $CaCO_3$ preservation, as reflected in the $CaCO_3$ MAR record. The first-order Pliocene-Pleistocene $CaCO_3$ MAR record trends from shallow sites of the California margin most likely reflect changes in $CaCO_3$ rain rate (production) rather than dissolution. Further work would be needed to assess the influence of other factors such as changes in bottom water chemistry and the influence of changes in lithology on the depth scale of oxic mineralization.

### 4.2. Middle Pliocene $CaCO_3$ Production

Modern ocean circulation and productivity along the California margin results from the North Pacific high-pressure regime. Seasonal fluctuations in the strength of the North Pacific high produces seasonal coastal upwelling, strongest in the north, and seasonal offshore upwelling, strongest in the southern California margin. Regions of coastal upwelling are characterized by high surface water nutrient content and cool temperatures. Offshore upwelling is characterized by a well-developed subsurface nutricline below relatively oligotrophic warm surface waters [*Ortiz et al.*, 1995]. *Chelton* [1982] found highest zooplankton volume in the surface waters in these offshore regions, particularly off southern California, associated with the maximum in the wind stress curl. A sediment trap study of modern $CaCO_3$ production in transects that span coastal, offshore (midway), and gyre hydrographic conditions demonstrates that the seasonal signal of $CaCO_3$ production offshore (midway) is linked to seasonal changes in offshore wind stress curl and is higher than $CaCO_3$ production in the coastal or gyre regions [*Lyle et al.*, 1992]. This model of $CaCO_3$ production offshore, where the subsurface position of the nutricline and relatively warm surface waters favors the proliferation of calcareous organisms, has been used to explain variations in Pleistocene paleoceanographic data from the northern region of the California Current system [*Ortiz et al.*, 1997]. The southern California margin, where the direction of the coastline deviates from the direction of the maximum winds, has a weaker seasonal expression. While these conditions produce less coastal upwelling relative to the northern California margin, they produce the strongest year-round offshore upwelling on the margin. Tanner Basin, the westernmost southern California Borderland basin drilled during Leg 167, is closest to the heart of this offshore upwelling zone. Basins located closer to shore (Sites 1011, 1012,and 1013) are influenced by the counter-current and gyre circulation of the Southern California Bight [*Hickey*, 1979].

The late Pleistocene pattern of $CaCO_3$ MAR (Figure 3a) consists of higher values in the California Borderland region and lower values at the seaward pelagic sites and at the northern sites. This first-order distribution can be explained by the dominance of offshore upwelling in the southern Borderland region in contrast to the northern California margin where coastal upwelling occurs at the nearshore sites and less intense seasonal offshore upwelling occurs at the offshore sites. During the middle Pliocene high $CaCO_3$ MAR event the geographical distribution of $CaCO_3$ MAR remains similar to that in the late Pleistocene, except that values at all sites are higher suggesting stronger offshore upwelling throughout the region (Figure 3). The signal is enhanced in California Borderland sites, particularly Site 1014, where conditions are particularly good for this type of upwelling. Enhanced offshore upwelling would have produced a shallower nutricline, more nutrient availability within the photic zone, and enhanced $CaCO_3$ production.

On a latitudinal transect of California margin Pliocene sediments, there are increases in the relative abundances of *Neogloboquadrina pachyderma* right-coiling (r.c), *Globigerina bulloides*, *Neogloboquadrina dutertrei/humerosa* complex, and *Globorotalia inflata/puncticulata* complex up to 47°N [*Ingle*, 1973a, b] approximately during the periods of high $CaCO_3$ MAR. Comparison to modern ground-truthing data from the Multitracers transect indicates that these species also have highest relative abundances in the offshore ("mid-way" between gyre and coastal environments) sediment traps [*Ortiz and Mix*, 1992] where $CaCO_3$ production is highest [*Lyle*, et al., 1992]. Therefore known changes in planktonic foraminifera distributions [*Ingle*, 1973a, b] through the Pliocene-Pleistocene are consistent with the idea that there were enhanced offshore upwelling, subsurface nutrient levels, and $CaCO_3$ production during the middle Pliocene; they also indicate that sea surface temperatures (SSTs)were warmer along much of the California margin (higher *N. pachyderma* (r.c.)) to (left-coiling(l.c.)ratio) [*Ingle* 1973b]. Thus, in addition to increased offshore upwelling, there were warmer SSTs because of to either a warming of the California Current subarctic source water and/or enhanced wind-driven shoreward mixing of warm subtropical gyral water.

The $CaCO_3$ MAR records from the California margin suggest that the surface wind field, particularly the offshore wind stress curl, was greater ~3.5-2.0 m.y. ago. These records therefore imply that eastern Pacific subtropical winds, and possibly the entire subtropical gyral circulation were stronger. This is supported by results from Leg 138 which predict that the Intertropical Convergence Zone (ITCZ) [*Hovan*, 1995] and associated hydrographic features [*Chaisson*, 1995; *Flores et al.*, 1995; *Hagelberg et al.*, 1995; *Cannariato and Ravelo*, 1997] shifted around 4.0 m.y. ago to a more southern position implying a strengthening of the northeast trades. If gyral circulation was strengthened during the period of high $CaCO_3$ MAR along the California margin 4.0-2.5 m.y. ago, the Kuroshio Current, the warm western boundary current of the North Pacific, may have also been enhanced. This is consistent with the idea that increased ocean heat transport may have played a role in explaining increased high-latitude surface temperatures of the middle Pliocene [*Crowley*, 1996; *Sloan et al.*, 1996]. Data-based studies [*Raymo et al.*, 1996; *van der Burgh et al.*, 1993] and modeling studies [*Crowley*, 1996; *Sloan* et al., 1996] indicate that in addition to increased ocean heat transport it is likely that at least slightly increased atmospheric $CO_2$ content in the middle Pliocene may have also contributed to observed climate changes. *Bakun* [1990]

suggests that increased greenhouse gas (GHG) concentrations since 1940 have produced a strengthening of the California Current; greater GHG concentrations cause enhanced continental heating of the western United States, a greater land-sea temperature contrast, and stronger wind-driven surface circulation. It may be that in the middle Pliocene, the eastern Pacific arm of the sub-tropical gyre responded to small changes in GHG content resulting in increased ocean heat transport thus acting as a positive feedback to enhance high-latitude warming.

Although the onset of the Pliocene $CaCO_3$ MAR event is approximately synchronous with northeast trade wind intensification and a southward displacement of the ITCZ [*Hovan*, 1995], the termination of the event at ~2.0 m.y. is not associated with a return of the ITCZ to its pre-Pliocene northern position. Rather, the termination must be associated with other Pacific climate events. The higher resolution records (Figure 4) show a two-step termination: the first step being synchronous with dramatic changes in the North Pacific during the transition to significantly larger northern hemisphere glaciations at 2.7 Ma [*Haug, et al.*, 1995]. This suggests that the termination of the $CaCO_3$ MAR event may be due to hydrographic changes associated with the reorganization of the North Pacific high-pressure system as glaciations increased in size. The final termination of the $CaCO_3$ MAR event at ~2.0 Ma, ~700,000 years after the end of the event in the North Pacific, may reflect the gradual establishment of a well-defined separation between the subtropical and subarctic gyres beginning at 2.7 Ma. At Site 882, in the subarctic gyre in the NW Pacific, the Pliocene high-carbonate event is also marked by high opal MARs and is a production event [*Haug et al.*, 1995 ]. On the California margin the high $CaCO_3$ MAR from 3.5 to 2 Ma may be caused by the extension of the subarctic high $CaCO_3$ production event into the region of the California margin combined with better $CaCO_3$ preservation until 2 Ma. However, high $CaCO_3$ MARs between 3 and 2 Ma along the California margin are independent of water depth, so $CaCO_3$ production must also be an important factor during this time period. Why $CaCO_3$ production along the California margin would lag $CaCO_3$ production in the NW Pacific is unclear.

Within the California margin sites there are some regional differences in the exact timing of the onset and termination of the high Pliocene $CaCO_3$ MAR event. At this point, without more detailed data, we can only speculate about the reasons for these regional differences. Relative to the most centrally located sites (1014, 1016, and 1018), the Southern Borderland sites (Site 1011, 1012,and 1013) have a broader Pliocene $CaCO_3$ MAR event with a gradual termination. This is probably due to the somewhat unique circulation of the Southern California Bight (SCB) gyre which recirculates southward flowing water back to the north in a countercurrent. Offshore upwelling in the SCB gyre may, in detail, have a different response to changes in the development of the North Pacific high than the rest of the California Current system. Relative to the most centrally located sites (1014, 1016, and 1018), the southernmost site (Site 1010) has a Pliocene $CaCO_3$ MAR event that begins and ends about 0.5 M.y. earlier. Site 1010 is the most likely site to be influenced by tropical climate changes, and the timing of the beginning of the event is actually in closest agreement with the timing of the southward shift of the ITCZ [*Hovan*, 1995]. Relative to the most centrally located sites (1014, 1016, and 1018), the northernmost sites (Sites 1020 and 1021), as well as the North Pacific site (Site 882, Figure 4) have their maximum $CaCO_3$ MAR values centered about 0.5 m.y. earlier, probably because they are readily affected by shifts in the transition between the subarctic and subtropical gyres. It may be that changes in the latitude of the transition zone at ~3.0 Ma caused a decrease in offshore upwelling and $CaCO_3$ production at these northern sites, while Pliocene $CaCO_3$ production remained high in the central sites until at least 2.5 Ma. Again, these speculations on the source of regional differences in the exact timing of the Pliocene $CaCO_3$ MAR event need to be supported by improved age models and by detailed records of hydrographic conditions and possible secondary dissolution effects.

Many of the proposed hydrographic changes presented here to explain the Pliocene $CaCO_3$ MAR record from Leg 167 sites can be tested in postcruise work. Using the model put forward by work related to the Multitracers studies [*Lyle et al.*, 1992; *Ortiz et al.*, 1995, 1997], enhanced offshore upwelling and $CaCO_3$ production would be accompanied by relative increases in midway foraminifera species, and higher photic zone nutrient levels. The role of intermediate source waters to upwelling regions will also be explored. Analysis of a nearshore site could provide evidence for the character of coastal upwelling through the Pliocene. The measurement of dissolution indices could help to address the nature of secondary influences of dissolution on the detailed timing of the $CaCO_3$ MAR trends. High-resolution studies and improved age models will provide detailed histories of the timing and sensitivity of the California current system to high-frequency variations in ice volume and insolation as climate evolved through the Pliocene.

## 5. Summary

Shipboard age models and measurements of wt % $CaCO_3$ and bulk density provide an estimate of Pliocene-Pleistocene $CaCO_3$ MARs along the California margin. There is a pattern of high $CaCO_3$ MARs in the middle Pliocene throughout the region. Although improved age models may improve our estimates of the magnitude and detailed timing of the $CaCO_3$ MAR event, the current age models are sufficiently robust to determine that a greatly expanded sequence with high $CaCO_3$ MAR was deposited in the middle Pliocene. The fact that both shallow and deep sites have similar patterns of $CaCO_3$ MAR suggests that the middle Pliocene was a period of enhanced $CaCO_3$ production. This is supported by the fact that neither the record of open Pacific CCrD fluctuations nor organic matter MAR correspond to the first-order trends in $CaCO_3$ MAR along the California margin. There are regional differences in the timing and duration of the high $CaCO_3$ MAR event along the California margin which are probably related to differences in hydrographic regime; northern sites are probably more sensitive to shifts in the transition between the subarctic and subtropical gyres, southern California Borderland sites are probably influenced by the evolution of the countercurrent and the gyre circulation within the Southern California Bight.

Studies of the modern distribution of $CaCO_3$ MAR across the California current [*Lyle et al.*, 1992] show that the highest $CaCO_3$ MAR is associated with offshore upwelling in the zone of the maximum wind stress curl. Thus the middle Pliocene

high $CaCO_3$ MAR event probably represents a period of enhanced wind stress curl and offshore upwelling. This suggests that the middle Pliocene, possibly a period of sustained high-latitude warmth relative to today, had stronger subtropical circulation and thus meridional heat transport in the north Pacific.

**Acknowledgments**. We would like to thank L. Peterson, three anonymous reviewers, and Associate Editor K. Miller for their insightful and thorough reviews which were extremely helpful when revising the manuscript. Many thanks go to the staff and technicians of Ocean Drilling Program Leg 167.

## References

Abelmann, A., R. Gersonde, and V. Spiess, Pliocene-Pleistocene paleoceanography in the Weddell Sea: Silicious microfossil evidence, in*Geological History of the Polar Oceans: Arctic Versus Antarctic* , edited by: U. Bleil and J. Thiede, pp.729-759, Kluwer Acad.,Norwell, Mass., 1990.

Archer, D., Modeling the calcite lysocline, *J. Geophys. Res.*, *96*, 17,037-17,050,1991.

Barron, J. A., Pliocene paleoclimatic interpretation of DSDP site 580 (NW Pacific) using diatoms, *Mar. Micropaleontology*, *20*, 23-44, 1992a.

Barron, J. A., Paleoceanographic and tectonic controls on the Pliocene diatom record of California, in *Pacific Neogene*, edited by R. Tsuchi and J. C. Ingle Jr.,pp. 25-42, Univ. of Tokyo Press, Tokyo, Japan, 1992b.

Barron, J. A., High resolution diatom paleoclimatology of the middle part of the Pliocene of the northwest Pacific, edited by D. K. Rea,et al,*Proc. Ocean Drilling Program, Sci. Results, 145,. 43-53,1995.*

Bakun, A., Global climate change and intensification of coastal upwelling, Science, 1990.

Bakun, A. and C. S. Nelson, The seasonal cycle of wind-stress curl in subtropical eastern boundary current regions, *J. Phys. Oceanogr.*, *21*, 1815-1834, 1991.

Berger, W. H., L. W. Kroenke, L. A. Mayer, and the Shipboard Scientific Party, Ontong Java Plateau, Leg 130: Synopsis of major drilling results, edited by L. W. Kroenke, et al., *Proc. Ocean Drilling Program, Initial Rep., 130*, 497-548, 1991.

Burkle, L. H., Calcium carbonate, biogenic opal and (Ge/Si) opal as climate indicators in the early Pliocene sediments of the Southern Ocean, *Mar. Micropaleontology.*, *27*, 215-226,1996.

Cande, S., and D. Kent, Revised calibration of the geomagnetic polarity timescale for the Late Cretaceous and Cenozoic, *J. Geophys Res.*, *100*, 6093-6095, 1995.

Cannariato, K., and A. C. Ravelo, Plio-Pleistocene evolution of eastern tropical Pacific surface water circulation and thermocline depth, *Paleoceanography*, in press,1997.

Chaisson, W. P., Population counts of planktonic foraminifera at four equatorial Pacific sites A comparison of west (Leg 130) and east (Leg138), latest Miocene to Pleistocene, edited by Pisias, N.G., et al., *Proc. Ocean Drilling Program, Sci. Results, 138*, 555-597, 1995.

Chelton, D. B., Large-scale response of the California Current to forcing by the wind stress curl, *California Cooperative Fisheries Investigations*, Rep. *XXIII*, pp.130-148, 1982.

Chelton, D. B., P. A. Bernal, and J. A. McGowan, Large-scale interannual physical and biological interaction in the California Current, *J Mar. Res.*, *40*, 1095-1125, 1982.

Ciesielski, P. F., and G. P. Grinstead, Pliocene variations in the position of the Antarctic Convergence in the southwest Atlantic, *Paleoceanography*, *1*, 197-232, 1968.

Ciesielski, P. F., and F. M. Weaver, Early Pliocene temperature changes in the Antarctic seas, *Geology*, *2*, 511-515, 1974.

Crowley, T. J., Pliocene climates: The nature of the problem, *Mar. Micropaleontology*, *27*, 3-12, 1996.

Defense Mapping Agency Hydrographic/Topographic Center, 1989. Sailing Directions (Planning Guide) for the North Pacific Ocean (3rd ed.): DMA Publication 152.

Dowsett, H. J. and R. Z. Poore, Pliocene sea surface temperatures of the North Atlantic Ocean at 3.0 Ma, *Quat. Sci. Rev.*, *10*, 189-204,1991.

Dowsett, H. J., T. Cronin, R. Poore, R S. Thompson, R. C. Whatley, and A M. Wood, Micropaleontological evidence for increased meridional heat transport in the North Atlantic Ocean during the Pliocene, *Science*, *258*, 1133-1134, 1992.

Emerson, S., and M. Bender, Carbon fluxes at the sediment-water interface of the deep-sea calcium carbonate preservation, *J. Mar. Res.*, *39*, 139-162, 1981.

Farrell, J. W. and W.L Prell, Pacific $CaCO_3$ preservation and $\delta^{18}O$ since 4 Ma: Paleoceanic and paleoclimatic implications, *Paleoceanography*, *6*, 486-498, 1991

Farrell, J. W., I. Raffi, T. R. Janecek, D. W. Murray, M. Levitan, K A. Dadey, D-C Emeis, M Lyle, J-A. Flores, and S. Hovan, Late Neogene sedimentation patterns in the eastern equatorial Pacific Ocean, edited by N.G.Pisias, et al., *Proc. Ocean Drilling Program, Sci. Results, 138:*, 717-753, 1995.

Flores, J.-A., F J. Sierro, and I. Raffi, Evolution of the calcareous nannofossil assemblage as a response to the paleoceanographic changes in the eastern equatorial Pacific from 4 to 2 Ma (Leg 138, Sites 849 and 852), edited by N G. Pisias, et al., *Proc Ocean Drilling Program, Sci. Results, 138,* 163-176, 1995.

Hagelberg, T. K., N. G. Pisias, L. A. Mayer, N. J. Shackleton, and A. C. Mix, Spatial and temporal variability of late Neogene equatorial Pacific carbonate, edited by N. G Pisias, et al., *Proc Ocean Drilling Program, Sci. Results, 138:*, 321-336, 1995.

Haug, G. H., M. A. Maslin, M. Sarnthein, R. Stax, R., and R.Teidemann, Evolution of northwest Pacfic sedimentation parterns since 6 Ma (Site 882), edited by D. K. Rea, I. A., Basov, D. W. Scholl, and J. F. Allan (Eds), *Proc. Ocean Drilling Program, Sci. Results, 145'*, 293 - 314, 1995.

Heusser, L. E., and J. J. Morley, Pliocene climate of Japan and environs between 4.8 and 2.8 Ma: a joint pollen and marine faunal study, *Mar. Micropaleontology*, *27*, 85-106, 1996.

Hickey, B. M., The California Current system hypotheses and facts, *Prog. Oceanogr.*, *8*, 191-279, 1979.

Hodell, D., and J. P Kennett, Late Miocene-early Pliocene stratigraphy and paleoceanography of the South Atlantic and southwest Pacific Oceans: A synthesis, *Paleoceanography*, *1*, 385-311, 1986.

Hodell, D., and K. Venz, Toward a high-resolution stable isotopic record of the Southern Ocean during the Plio-Pleistocene (4.8- 0.8 Ma), in *The Antarctic Paleoevironment: A Perspective on global change, Antarct. Rese. Ser* , vol 56, edited by J. P. Kennett and D. A. Warnken, pp. 265-310, AGU, Washington, D. C., 1992.

Hodell, D., and D. A. Warnke, Climate evolution of the Southern Ocean during the Pliocene epoch from 4.3 to 2.6 million years ago, *Quat. Sci. Rev.*, *10*, 205-214, 1991.

Hovan, S. A., Late Neogene atmospheric circulation intensity and climatic history recorded by eolian deposition in the eastern equatorial Pacific, ODP Leg 138, edited by N G Pisias, et al., *Proc.Ocean Drilling Program, Sci. Results, 138*, 615-626, 1995.

Huyer, A., Coastal upwelling in the California Current system *Prog. Oceanogr.*, *12*, 259-284, 1983.

Ingle, J. C., Neogene foraminifera from the northeastern Pacific Ocean, Leg 18, Deep Sea Drilling Project, edited by L C. Kulm, et al., *Initial. Rep. Deep Sea Drill. Proj.*, *18*, 517-568, 1973a.

Ingle, J. C., Summary comments on Neogene biostratigraphy, physical stratigraphy, and paleoceanography in the marginal northeastern Pacific Ocean, edited by L. C. Kulm, et al , *Initial Rep. Deep Sea Drill. Proj.*, *18*, 949-961,1973b.

Jahnke, R.A., Early diagenesis and recycling of biogenic debris at the seafloor, Santa Monica Basin, California, *J. Mar. Res.*, *48*, 413-436, 1990.

Karlin, R., M Lyle, and R. Zahn, Carbonate variations in the NE Pacific during the late Quaternary. *Paleoceanography*, *7*, 43-63, 1992.

Kutzbach, J. E., Model simulations of the climatic patterns during the deglaciation of North America, edited by W. F. Ruddiman, and H. E Wright Jr., *North America and Adjacent Oceans During the Last Deglaciation., The Geology of North America*, vol K-3, 425-447, Geol. Soc of Am., Boulder, Colo., 1987.

Kutzbach, J. E., P. J. Guetter, P Behling, R. and Selin, Simulated climatic changes: results of the COHMAP climate-model experiments, edited by H.E. Wright Jr., et al.,*Global Climates Since the Last Glacial Maximum: Minneapolis* , Univ. of Minn. Press, 24-94, 1993.

Lyle, M., I. Koizumi, C. Richter, and the Shipboard Scientific party, *Procedings of the Ocean Drilling Project, Initial Reports, vol.* 167, *Ocean Drilling Program*, College Station, Tex, 1997.

Lyle, M., R. Zahn, F. Prahl, J. Dymond, R Collier, N Pisias, and E. Suess, Paleoproductivity and carbon burial across the California Current: The MULTITRACERS transect, 42°N, *Paleoceanography*, *7*, 251-272, 1992.

Lynn, R. J., and J. J. Simpson, The California Current system: The seasonal variability of its physical characteristics, *J. Geophys Res* , *92*, 12,947-12, 1987.

Mayer, L., N. Pisias, T. Janecek, and the Leg 138 Shipboard Scientific Party, Site 846, *Proc. Ocean Drilling Program, Initial Rep , 138:*, 265-334, 1992.

Ortiz, J. D., and A C. Mix, The spatial distribution and seasonal succession of planktonic foramminifera in the California Current off Oregon, September 1987-September 1988, *Upwelling Systems. Evolution since the Early Miocene*, edited by C. P. Summerhayes, W. L. Prell, K. C. Emeis, Spec. Publ. 64, Geol. Soc., pp.197-214, London,1992.

Ortiz, J. D., A. C. Mix, and R. W. Collier, Environmental control of living symbiotic and asymbiotic foraminifera of the California Current, *Paleoceanography*, *10*, 987-1009, 1995.

Ortiz, J. D., A. Mix, S. Hostetler, and M Kashgarian, The California Current of the last glacial maximum: Reconstructions at 42°N based on

multiple proxies, *Paleoceanography, 12*, 191-206, 1997.

Pares-Sierra, A., and J. J. O'Brien, The seasonal and interannual variability of the California Current system: A numerical model, *J. Geophys. Res.*, 94, 3159-3181, 1989.

Peterson, L. C., D. W. Murray, W. U Ehrmann, and P. Hempel, Cenozoic carbonate accumulation and compensation depth changes in the Indian Ocean. *Synthesis of Results From Scientific Drilling in the Indian Ocean, Geophys. Monogr.* 70, edited by R. Duncan and D. Rear, pp. 311-333, AU, Washington, D. C.,1992.

Raymo, M. E., G. Grant, M. Horowitz, and G. H Rau, Mid-Pliocene warmth: Stronger greenhouse and stronger conveyer, *Mar. Micropaleontology, 27*, 313-326, 1996.

Rind, D., and M. Chandler, Increased ocean heat transports and warmer climate, *J. Geophys. Res.*, *96*, 7437-7461, 1991.

Sloan, L. C., T. J. Crowley, and D. Pollard, Modeling of middle Pliocene climate with NCAR GENESIS general circulation model. *Mar. Micropaleontology, 27*, 51-61, 1996.

van der Burgh, J., H. Visscher, D. L. Dilcher, and W. M. KurscherPaleoatmospheric signatures in Neogene fossil leaves, *Science, 260*, 1788-1790, 1993.

J P. Caulett, Laboratoire de Geologie, Museum National d'Histoire Naturelle, Paris 75005, France.

E. Fornaciari, Dipartimento di Geologia, Paleontologiia e Geofisica, Universita degli Studi de Padova, Padova 35137, Italy.

A. Hayashida, Science and Engineering Research Institute, Doshisha University, Tanabe 610-03, Japan.

F. Heider, Institut for Gephysik, Universitat Munchen, Munchen 80333, Germany.

J. Hood and A. Janik, MGG/RSMAS, University of Miami, Miami, FL 33149-1098..

S. Hovan, Geosciences Department, Indiana State University of Pennsylvania, Indiana, PA 15705-11087.

T. Janeck, Antartic Research Facility, Department of Geology, Florida State University, Tallahassee, FL 32306.

I. Koizumi, Division of Earth and Planetary Sciences, Hokkaido University, Sapporo 060, Japan.

M. Lyle, CGISS, Boise State University, Boise, ID 83725.

A. C. Ravelo, Institute of Marine Sciences, University of California, Santa Cruz, CA 95064. (e-mail: acr@aphrodite.ucsc.edu)

R. Stax, Institute for Geology and Mineralogy, University of Erlangen, Erlangen 91054, Germany.

M. Yamato, Fuel Resources Department, Geological Survey of Japan, Tsukuba 305, Japan.

(Received March 3, 1997;
revised August 15, 1997;
accepted September 8, 1997.)